

Formation and Alignment of Z Lines in Living Chick Myotubes Microinjected with Rhodamine-labeled Alpha-Actinin

Nancy M. McKenna,* Catharine S. Johnson,* and Yu-li Wang*‡

*Department of Molecular and Cellular Biology, National Jewish Center for Immunology and Respiratory Medicine, Denver, Colorado 80206; ‡Department of Biochemistry, Biophysics and Genetics, University of Colorado Health Sciences Center, Denver, Colorado 80220

Abstract. We have used fluorescence analogue cytochemistry in conjunction with time lapse recording to study the dynamics of alpha-actinin, a major component of the Z line, during myofibrillogenesis. Rhodamine-labeled alpha-actinin microinjected into living cultured chick skeletal myotubes became localized in discrete cellular structures within 1 h and remained specifically associated with structures for up to 4 d, allowing individual identified structures to be followed during development. In the most immature cells used, alpha-actinin was found in diffuse aggregates, some of which displayed sarcomeric periodicity. Aggregates were observed to coalesce into better defined structures (Z bands) that were $\sim 1.0\text{-}\mu\text{m}$ wide. Z bands condensed into narrow, more intensely fluorescent Z lines in 4–48 h. During this period, Z lines grew laterally, primarily by the addition of small beads of

alpha-actinin to existing Z lines or by the merging of small Z lines. In more mature cells, alpha-actinin added to Z lines without going through a visible intermediary structure. Mean sarcomere length did not change significantly during the stages examined, although the variability of sarcomere length did decrease markedly over time for identified sets of sarcomeres. At early stages, myofibrils frequently shifted position in both the longitudinal and lateral directions. Neighboring myofibrils were frequently associated for one or more sarcomeres sporadically along their length, such that the intervening sarcomeres were often misaligned. Associations between myofibrils were often transitory. Shifts in myofibril location in conjunction with the formation, breaking, and reformation of lateral associations between myofibrils facilitated the alignment of Z lines through a trial and error process.

MATURE striated muscle cells are densely packed with almost perfectly aligned myofibrils. The formation of these myofibrils represents one of the most dramatic examples of macromolecular assembly in eukaryotic cells. Under most conditions, myofibrillogenesis occurs after the fusion of myoblasts and the coordinate initiation of synthesis of muscle-specific contractile proteins (3, 10). The first indications of myofibrillogenesis detectable with the electron microscope are small bundles of actin and myosin filaments, already arranged in the regular double hexagonal pattern characteristic of sarcomeres (see references 13 and 14). Diffuse structures, which are presumably precursors of Z lines and have been referred to as "Z-bodies" (21), appear to associate with these small filament bundles; definite, although ragged, Z lines, are present on larger bundles. At later stages, sarcomeres are well-defined and similar to those observed in mature muscle.

Despite these detailed studies, little is known about how structures present at early stages are related to well-organized myofibrils in mature myotubes. One major limitation has been the static nature of the data obtained using conventional approaches such as electron microscopy and immunofluorescence. Although many descriptions of the mor-

phology of structures and the localization of proteins are available (see for example, 1, 2, 5, 6, 13, 14, 15, 17, 19, 21, 24, 29, 32, 36), it has not been possible to develop a definitive picture of the dynamic events of development. In addition, it has been difficult to establish directly the interrelationships of structures in different parts of the cell with electron microscopic techniques, since only a very small section of the cell can be examined at one time.

We have used fluorescence analogue cytochemistry in conjunction with time-lapse recording to study the dynamics of alpha-actinin containing structures during myofibrillogenesis in living cultured chick myotubes. Alpha-actinin was the protein of choice for several reasons. It has been studied in detail biochemically and permits a functional assay in vitro of the fluorescently labeled conjugate (16). It can also be easily visualized after microinjection since it is concentrated in a small well-defined structure, the Z line (7, 8, 25). Although stress fiber-like structures (5, 29) or acto-myosin bundles (10, 11) may be the primary organizing component in the initial steps of sarcomerogenesis, there is little doubt that the Z line and its precursors play an important role in both the formation and maintenance of sarcomere structures. For example, Peng et al. have suggested that the formation of sarco-

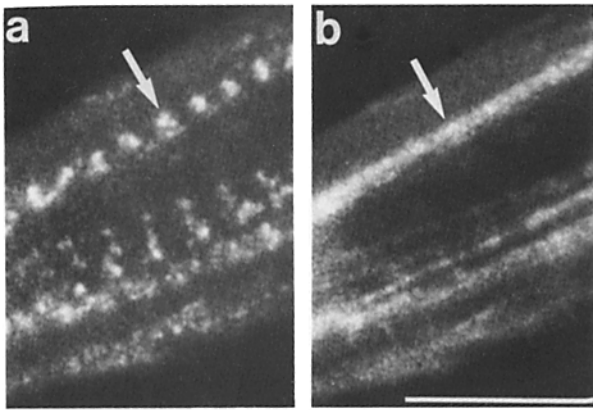


Figure 1. Comparison of microinjected rhodamine alpha-actinin and fluorescein phalloidin in a relatively immature myotube from a 7-d culture. Cells injected with rhodamine alpha-actinin were fixed, extracted, and stained with fluorescein phalloidin. Comparison of the rhodamine alpha-actinin image (*a*) of the fixed cell with the fluorescein phalloidin image (*b*) indicates that wide bands of alpha-actinin ($0.63 \pm 0.02 \mu\text{m}$) are associated with apparently continuous actin fibers. However, increased phalloidin fluorescence is detectable in the same locations as alpha-actinin (*arrow*) along the upper fibril. Bar, $10 \mu\text{m}$.

meres of a well-defined length is coincident with the formation of Z lines (29). Other authors have reported that the disorganization of Z lines is one of the earliest effects of 12-O-tetradecanoylphorbol-13-acetate, which causes disassembly of myofibrils (9, 11). Similarly, the partial breakdown of myofibrils that occurs in dividing cardiac cells is also preceded by the disappearance of the Z line (21).

In this study, we have focused on two major questions: how diffuse aggregates of alpha-actinin in immature cells are related to Z lines in mature myotubes and how myofibrils attain their high degree of lateral alignment. We demonstrate that diffuse alpha-actinin containing aggregates can directly develop into Z lines through coalescence and condensation. In addition, we show that the highly dynamic character of nascent myofibrils allows alignment to be achieved through a trial and error process.

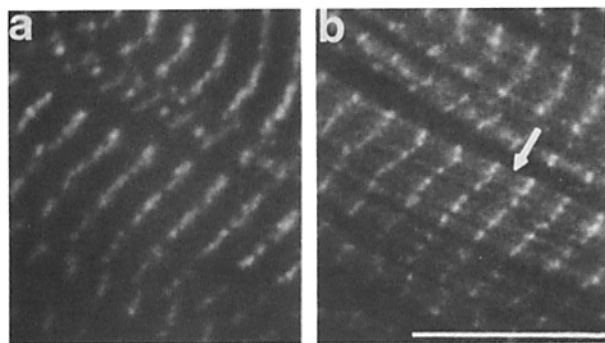


Figure 2. Comparison of microinjected rhodamine alpha-actinin and fluorescein phalloidin of a mature myotube from an 8-d culture. In this cell, rhodamine alpha-actinin (*a*) is localized in narrow, well-defined Z lines ($0.37 \pm 0.02 \mu\text{m}$) which are aligned laterally. Phalloidin (*b*) stains the I bands and the Z lines, whereas the M lines are visible as dark lines (*arrow*). The phalloidin-stained Z lines are quite narrow ($0.30 \pm 0.03 \mu\text{m}$). The phalloidin image also reveals that many small myofibrils comprise each broad myofibril. Bar, $10 \mu\text{m}$.

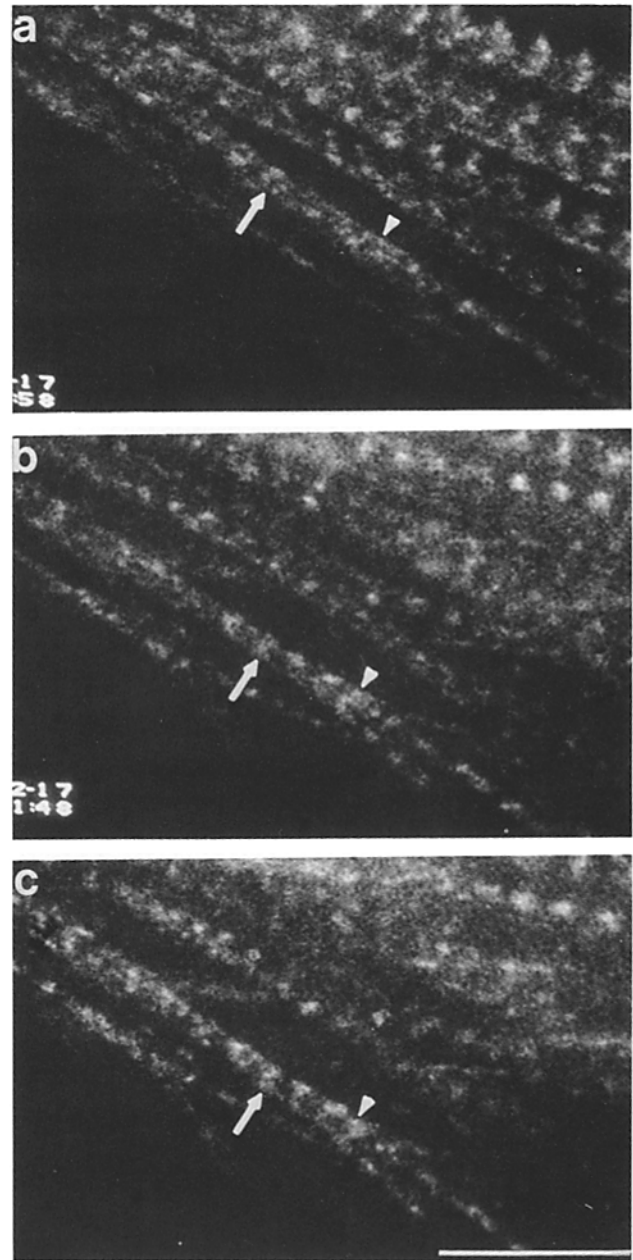


Figure 3. Coalescence of alpha-actinin aggregates into periodic bands in a rhodamine alpha-actinin injected myotube from a 6-d culture. The arrows indicate the same Z bands at each time point. In *a*, alpha-actinin is localized in many irregular aggregates or beaded structures along a fibril. The arrowhead points to a small, relatively discrete, bead of alpha-actinin. Wispy threads of alpha-actinin connect this bead with nearby aggregates. After $3\frac{1}{2}$ h (*b*), the bead (*arrowhead*) has become part of one of the larger, diffuse aggregates. These large aggregates have a periodicity of $1.87 \pm 0.10 \mu\text{m}$. At 5 h (*c*), the large aggregates are organized into bright bands $0.76 \pm 0.06 \mu\text{m}$ wide, which have a periodicity of $1.86 \pm 0.08 \mu\text{m}$. The bead (*arrowhead*) can still be discerned in one of the large aggregates. Bar, $10 \mu\text{m}$.

Materials and Methods

Preparation of Fluorescent Analogues

Smooth muscle alpha-actinin was isolated from frozen chicken gizzards and labeled with tetramethylrhodamine as described previously (27).

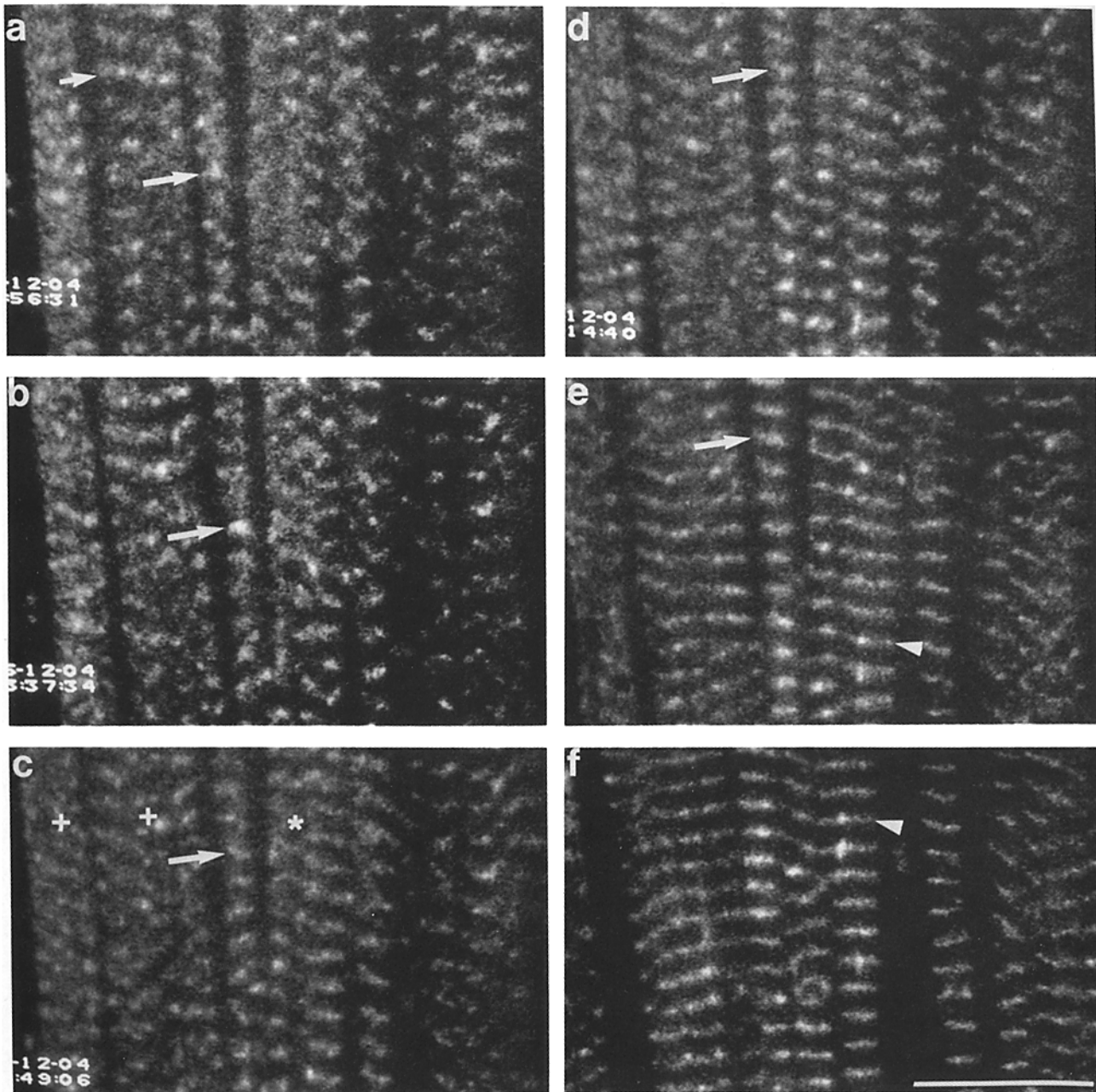


Figure 4. Condensation of alpha-actinin in a 7-d myotube. Long arrows indicate the same Z band/Z line in *a-e* and arrowheads indicate the location of a single Z line in *e* and *f*. In *a*, alpha-actinin is localized in diffuse beads which seem to be organized into longitudinal structures of varying widths. Some beads (*short arrow*) are laterally associated. At 1½ h (*b*), more beads have become laterally associated into broad irregular bands, which are $1.04 \pm 0.07\text{-}\mu\text{m}$ wide and have a periodicity of $1.94 \pm 0.11\text{ }\mu\text{m}$. At 4 h (*c*) and 5 h (*d*), the organization of alpha-actinin into broad bands has become more distinct. In *c*, the mean width of the alpha-actinin bands is $0.83 \pm 0.03\text{ }\mu\text{m}$. The fibrils on the left (+) have increased considerably in width, and the wide fibril in the center (*) seems now to be clearly composed of several smaller myofibrils. By 10 h (*e*), the broad bands have condensed down to $0.57 \pm 0.03\text{ }\mu\text{m}$ so that the Z lines appear to be well-defined and regular. The beaded nature of the bands has also become less prominent. At 21 h (*f*), alpha-actinin is localized in narrow, $0.43 \pm 0.03\text{ }\mu\text{m}$ Z lines. The sarcomeric periodicity, $1.87 \pm 0.05\text{ }\mu\text{m}$, is essentially the same as in *b*. The Z lines of adjacent myofibrils are well-aligned, although some mismatches are present. Note the changes in the positions and lateral associations of myofibrils throughout this sequence. This cell was observed for 36 h more, during which time additional maturation, such as alignment and increases in myofibril width (see Fig. 10), occurred. Bar, 10 μm .

Cell Culture, Microinjection, and Fluorescence Microscopy

Muscle cell cultures were obtained from leg muscle of 11-d chick embryos by mechanical dissociation (22). Cells were plated on collagen-coated cover slips with densities between 4×10^3 and 9×10^3 cells per 35-mm dish and maintained in Eagle's minimum essential medium (KC Biological Inc.,

Lenexa, KS) with 10% horse serum (KC Biological Inc.), 2% embryo extract, penicillin, and streptomycin at 38°C. This medium produced cultures of small, discrete myotubes. 2 d after plating, cytosine arabinofuranoside (Sigma Chemical Co., St. Louis, MO) was added to most cultures to decrease fibroblast contamination. No differences in developmental processes were detected when myotubes in untreated cultures and cytosine arabinofuranoside-treated cultures were compared.

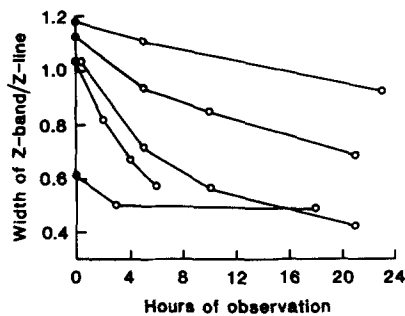


Figure 5. Decrease in width of Z bands/Z lines with time for five typical cells. The width of each fluorescent Z band/Z line was measured as described in Materials and Methods. The same Z bands/Z lines were measured at each time point for each cell and the mean plotted. Error bars are not shown, but all standard errors were $<0.04 \mu\text{m}$. The rate of narrowing seems to level off when the width of the Z line reaches $\sim 0.5\text{--}0.6 \mu\text{m}$, but the Z lines continue to narrow slowly to $\sim 0.35\text{--}0.40 \mu\text{m}$ in mature myotubes.

5–8 d after plating, cells were microinjected as described previously (26). Some cells contracted upon injection. The volume of protein injected was estimated to be 5–10% of the cell volume (39). Variations in injection volume did not affect results. The distribution of smooth muscle alpha-actinin has been shown to mimic closely the distribution of endogenous alpha-actinin in several systems (12, 33). After microinjection, cells were incubated 4–18 h to allow incorporation of the injected analogue into cellular structures. Individual cells were followed for 5–72 h during which time fluorescently labeled alpha-actinin remained incorporated in cellular structures and cells appeared healthy with phase microscopy. Localization of alpha-actinin differed depending on the age and developmental stage of the cell, which in turn depended on culture conditions and cell density. The extent of sarcomere development often varied from cell to cell on the same plate and even in different regions of the same cell.

Observation of culture dishes was carried out on the heated, humidified stage of a Zeiss IM-35 inverted microscope with supplemental CO_2 . A $100\times$ Neofluar oil immersion objective (1.30 numerical aperture) and epillumination were used. A 100-W quartz halogen lamp was used as a light source and operated at 4–6 V. The low level of light did not cause any detectable cell damage.

Fixation and phalloidin staining were carried out as described by Amato et al. (4) with fluorescein phalloidin (Molecular Probes Inc., Eugene, OR). To avoid crossover of rhodamine fluorescence into the fluorescein image, an extra filter was added (cutoff wavelength 550 nm).

Image Processing and Analysis

Hardware used for detection of fluorescent images was identical to that described previously (26). Acquisition of images during an experiment was carried out by feeding raw images from the image intensifier into the image processing system, which averaged 128 successive frames and subtracted

the image of the dark current to remove background before storage on the hard disk. Gain and high voltage settings on the image intensifier were left constant and gamma correction was disabled for all experiments.

The experimental procedure involved searching the plate by eye to find an injected cell at the desired developmental stage. Once a cell was chosen, the stage was kept stationary to ensure that the same area of the cell was observed. Images of the cell were recorded every $\frac{1}{2}$ –12 h for up to 72 h.

Distances were measured by denoting points on the displayed image with the use of a graphics tablet (GTCO, Rockville, MD) and then calculating the distance based on the number of pixels between points, accounting for the rectangular shape of the pixel. For the $100\times$ objective, each pixel is equivalent to an area of $0.1 \times 0.08 \mu\text{m}$. Sarcomere length was calculated by measuring from the center of one Z line/Z band to the center of the next Z line/Z band. Measurements of fluorescence intensity were obtained by averaging the pixel intensities of an area delimited with the tablet. Results are reported as means plus or minus standard error, except where noted otherwise. We used the paired *t* test for statistical analysis of the data.

Since fluorescence microscopy tends to overstate the actual size of an object, we examined the images of $0.3\text{-}\mu\text{m}$ polystyrene beads labeled with fluorescein (Covalent Technology, Ann Arbor, MI) under the same conditions as described above. At relatively low image intensities (31–45 units on a grey scale of 0–255), which were comparable to the usual intensities of alpha-actinin containing structures in our experiments, the mean apparent size of the $0.3\text{-}\mu\text{m}$ beads was $0.43 \mu\text{m}$ (SE = $0.02 \mu\text{m}$), whereas at higher intensities (131–158 units), which were comparable to the brightest structures encountered in these experiments, the mean apparent size was $0.56 \mu\text{m}$ (SE = $0.03 \mu\text{m}$). Therefore, our measurements of small fluorescent objects like the beads probably overestimate their true size by between 43 and 187%. For larger objects, the error should be smaller. Thus, the actual size of immature Z bands should be close to the measured size, while the actual size of mature, intensely fluorescent Z lines should be considerably smaller than the measured size. As a result, the extent of condensation, as shown in Fig. 5, is likely to be underestimated.

Results

Our experiments have focused on the developmental events that occur between days 5 through 8 under defined culture conditions. At all stages, microinjected alpha-actinin became localized in cellular structures within 1 h and reached an apparent steady state within 3–4 h. In the earliest stages examined (5–7 d in culture), myotubes observed by phase microscopy were narrow and short. Alpha-actinin microinjected into these immature myotubes localized in aggregates that had often attained sarcomeric periodicity, but were rarely aligned laterally. In the phalloidin image of this stage, actin was present in continuous linear structures with bands of increased fluorescence intensity occurring along some linear structures (Fig. 1). Between 6 and 7 d, myotubes were larger in phase microscopy and distinct sarcomeres were detectable in both alpha-actinin and phalloidin images. From 7 d on,

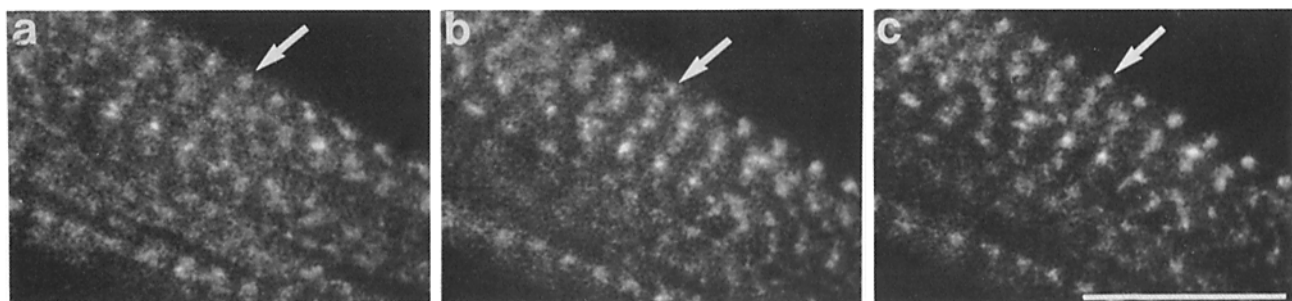


Figure 6. Increase in the intensity of alpha-actinin in periodic bands in a myotube from a 7-d culture. Arrows indicate the same Z band at each time point. At time 0 (a), diffuse bands of alpha-actinin are observed. 2 h later (b), the bands have condensed and become more fluorescent. By 3 h (c), the increase in the fluorescence of the bands relative to that of the spaces between the bands is even more pronounced. The ratios of the average fluorescence intensity of five bands to that of five spaces between the bands are 1.75 ± 0.14 for a, 2.04 ± 0.22 for b, and 2.30 ± 0.14 for c. Bar, $10 \mu\text{m}$.

Table I. Relationship between Decreases in Z Band/Z Line Width and Increases in Z Band/Z Line Fluorescence Intensity

Cell No.	Hours observed	Initial Z band/Z line width	Change in Z band/Z line width	Change in fluorescence intensity*
1023a	6	>0.75 μm	Decreases	Increases
1030	3			
0731	6			
0114a	23			
1204	20			
0910	8	<0.75 μm	Decreases	Increases,
0114b	12			
1204b	21			
1009	8			
0911	7			
1008	4			

Z band/Z line widths and intensities were measured as described in Materials and Methods. Values were analyzed using the paired *t* test. NS, not significant. * Fluorescence intensity is expressed as a ratio of the fluorescence intensity of the Z bands/Z lines divided by the fluorescence intensity of the region between the Z bands/Z lines.

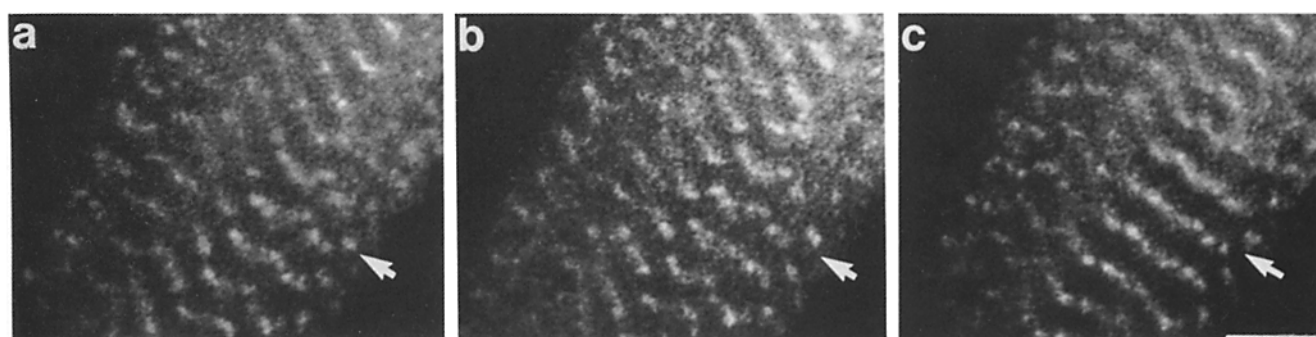


Figure 7. Straightening of Z lines in an alpha-actinin injected myotube from a 7-d culture. At time 0 (a), beads of alpha-actinin are laterally associated, but form a wavy ribbon (arrow). 35 min later (b), the Z line below the one indicated by the arrow has straightened out. At 70 min (c), the beads of the Z line indicated by the arrow have also formed a fairly straight line. Bar, 5 μm .

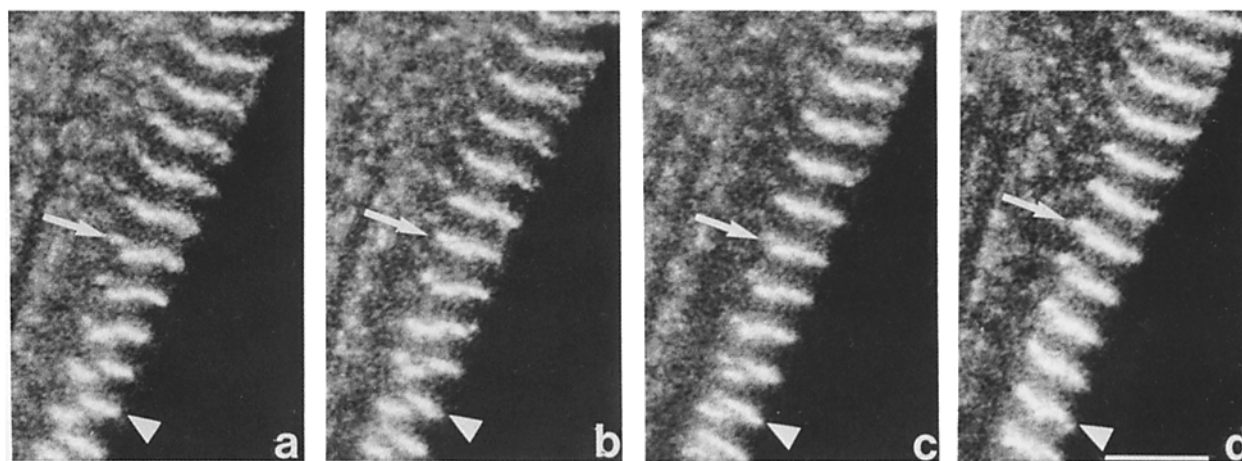


Figure 8. Recruitment and merging of alpha-actinin containing structures in 6-d-old myotube microinjected with alpha-actinin. At time 0 (a), several beads of alpha-actinin are close to, but not aligned with, Z lines (arrow). Lower down in the photograph, the Z lines of two small myofibrils are anti-periodic (arrowhead). At 1 h (b) and 1½ h (c), the beads have become more aligned with adjacent Z lines, while the Z lines of the small myofibrils in the lower part of the cell have moved closer together and overlap along their lengths. By 4 h (d), the beads have joined the adjacent Z lines, and most of the Z lines of the small myofibrils in the lower part of the cell have merged. Bar, 5 μm .

phase microscopy revealed large diameter myotubes that were sometimes cross-striated along part of their length. The alpha-actinin images of these mature myotubes showed large numbers of intensely fluorescent, well-aligned Z lines; phal-

loidin stained the Z lines and I bands, whereas the M lines were present as nonfluorescent bands (Fig. 2).

By storing images of a specific area in a single living cell every ½-12 h, we have been able to track individual ag-

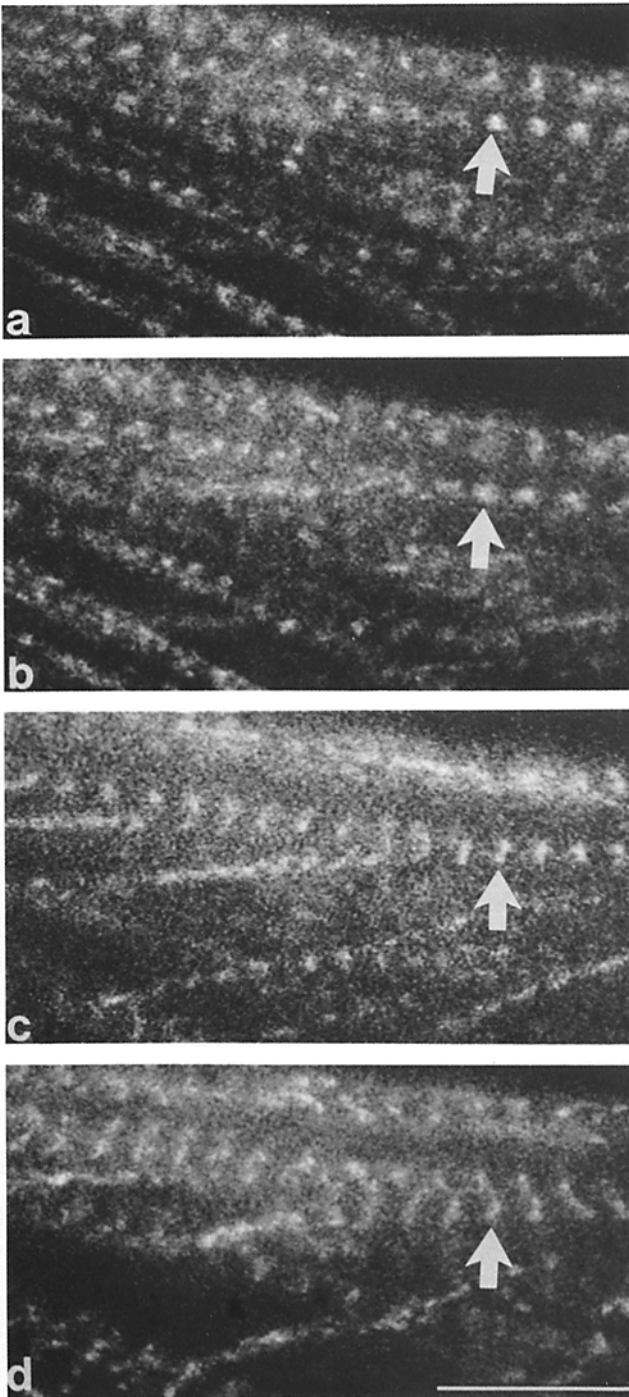


Figure 9 Simultaneous condensation of diffuse alpha-actinin and increase in Z band width. At 0 time (*a*), the width of the Z band indicated by the arrow is $0.77 \pm 0.05 \mu\text{m}$; its length (perpendicular to the long axis of the myofibril) is $0.73 \mu\text{m}$. $1\frac{1}{2}$ h later (*b*), the length of the Z band (and presumably the width of the myofibril) has increased slightly to $0.87 \mu\text{m}$. By $4\frac{1}{2}$ h (*c*), the Z line has condensed down to $0.46 \pm 0.05 \mu\text{m}$ and has increased in length to $1.43 \mu\text{m}$. At $18\frac{1}{2}$ h (*d*), the width of the Z line is still $0.46 \pm 0.03 \mu\text{m}$. The Z line length has increased substantially to $3.35 \mu\text{m}$. This sequence shows a section of the same myotube as in Fig. 3. *a* is the same time point as *b* in Fig. 3. Bar, $10 \mu\text{m}$.

gregates of alpha-actinin from the time that sarcomeric periodicity was recognizable through the organization of well defined, laterally aligned Z lines. Comparison of adjacent, unobserved cells at the end of each experiment indicated that the progress of myogenesis was not affected by observation. This was also confirmed by comparing the phalloidin-stained images of unobserved and observed cells and those of uninjected and injected cells (not shown).

Reorganization of alpha-actinin (for example, Figs. 3 and 4) in the most immature myotubes occurred through several processes. Diffuse aggregates of alpha-actinin were observed to coalesce with adjoining aggregates, forming a pattern of alternating fluorescent and nonfluorescent bands, in as little as 5 h (Fig. 3). From the time that they could first be detected, these bands were arranged in sarcomeric periodicity and were quite wide (Figs. 1 *a*, 3*b-c*, 4, and 9). Although the mean sarcomere length did not change, these wide Z bands gradually decreased in width from a maximum of $\sim 1 \mu\text{m}$ to $0.5 \mu\text{m}$ or less over 24–48 h (Figs 4, 5, and 9). Since fluorescence microscopy tends to overstate the actual size of objects (see Materials and Methods) these measurements must be considered in a relative sense, rather than as absolute values. We have termed the $0.75 \mu\text{m}$ or wider alpha-actinin containing structures which have sarcomeric periodicity, Z bands, and those narrower than $0.75 \mu\text{m}$, Z lines. As Z bands/Z lines became narrower, the ratio of the fluorescence intensity in Z bands/Z lines to the fluorescence intensity in the intervening regions increased significantly (Fig. 6, Table I). This suggests that the narrowing of Z bands was due to the condensation of diffuse alpha-actinin into more concentrated structures.

A second process that refines the Z band into the Z line is the increasingly lateral organization of alpha-actinin containing structures. In immature myotubes, Z lines often had the appearance of wavy ribbons. As the cells matured, the beads comprising the Z line became arranged in a much more linear pattern (Fig. 7). Coincidentally, Z lines also became much more perpendicular to the long axis of the myotube (see Fig. 12).

Throughout this period, Z bands/Z lines grew considerably in length (perpendicular to the long axis of the myofibril). Frequently, aggregates of alpha-actinin in less organized regions of the cell were recruited into adjoining myofibrils. As shown in Fig. 8, this process involved the movement of an independent aggregate closer to the Z line until they became indistinguishable. In addition to recruitment, short nascent Z lines could also align and merge to form longer Z lines (Fig. 8).

Recruitment and merging were generally observed only in relatively immature myotubes. A second method of lateral growth of Z lines—the direct addition of alpha-actinin to existing Z lines without the involvement of a visible intermediary structure—occurred in both immature (Fig. 9) and mature myotubes (Fig. 10).

During these stages of alpha-actinin reorganization, the mean sarcomere length did not change significantly for most of the cells followed. However, the variability of sarcomere length as indicated by the size of the standard deviation of the mean decreased significantly ($P < 0.05$, five cells) over time for identified sets of sarcomeres. The range in length for these sarcomeres was initially $1.32\text{--}2.97 \mu\text{m}$ (mean = $1.95 \mu\text{m}$, SD = 0.34 , $n = 30$); at the final time point 8–24

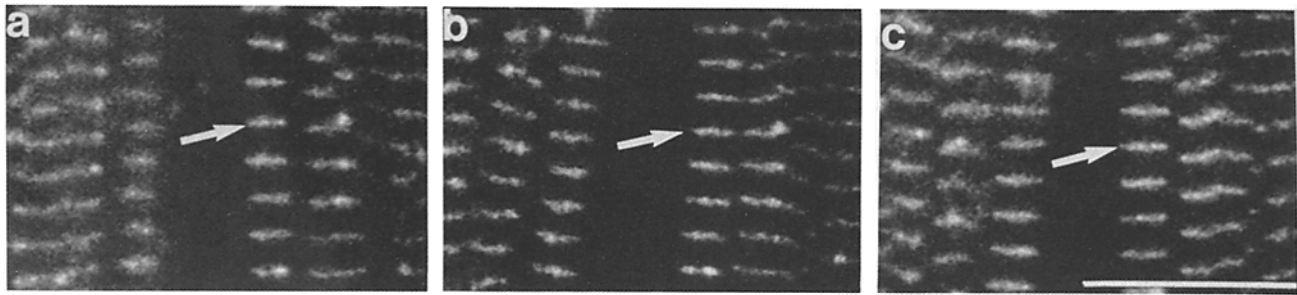


Figure 10. Increase in the length of Z lines in an alpha-actinin injected myotube, 8 d in culture. The length of the Z line at the point indicated by the arrow increases from 1.73 μm at time 0 (*a*) to 1.94 μm at 8 h (*b*) and to 2.23 μm at 25 h (*c*). Close examination of these images and of intervening time points indicates that alpha-actinin was added directly to Z lines without going through an intermediary structure such as beads. Note, too, that the sarcomeres immediately above the one indicated by the arrow have become aligned and laterally associated with sarcomeres of the neighboring myofibril in *b*. In *c* however, these sarcomeres have “unzipped” and are no longer aligned. This cell is the same cell as in Fig. 4, but 1 d later. Bar, 10 μm .

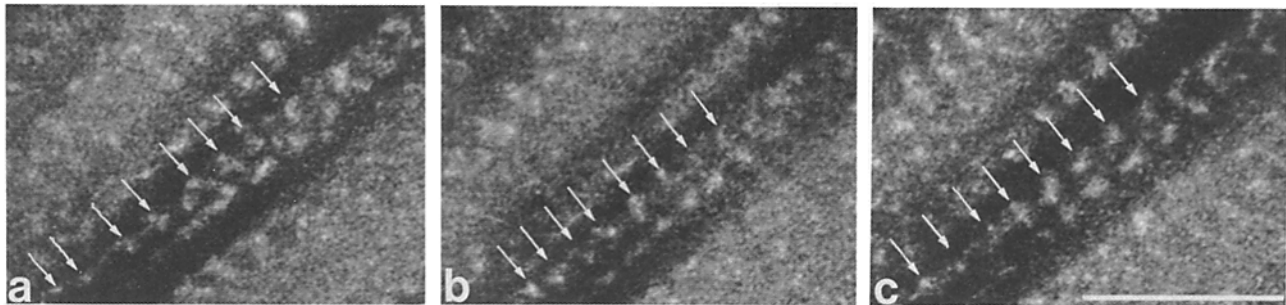


Figure 11. Decrease in the variability of sarcomeric periodicity in a myotube from a 7-d culture. Arrows indicate the same aggregates of alpha-actinin at each time point. In *a*, the distances between the aggregates are highly variable, ranging from 1.20 to 2.64 μm (mean = 1.93; SD = 0.47; $n = 7$). Some of the aggregates are connected by linear wisps of alpha-actinin. 2 h later (*b*), the spacing has changed; some aggregates have moved closer together, others have moved farther apart. The aggregates are now clearly organized into Z bands as well. By 4 h (*c*), an even more regular spacing (1.66–2.26 μm ; mean = 1.94; SD = 0.19; $n = 7$) is evident. Bar, 10 μm .

h later, the range was 1.6–2.32 μm (mean = 1.95, SD = 0.25, $n = 30$). This decrease in variability involved both increases and decreases in the length of individual sarcomeres (Fig. 11).

At early stages, when most myofibrils had relatively narrow widths, myofibrils frequently changed position within the cell (Figs. 3, 4, 9, 10, and 12), usually shifting longitudinally, but occasionally shifting laterally. At the same time, sarcomeres of neighboring fibrils often became associated at one or more points along their length. Such associations frequently involved just a few sarcomeres, but sometimes were quite extensive. When multiple associations were present, the number of sarcomeres between the areas of association were often different for the two myofibrils so that they were essentially misaligned (Fig. 12). Many of these early associations were short lived. For example, the two myofibrils shown in Fig. 12 dissociate (“unzip”) sarcomere by sarcomere (see also Fig. 10). This unzipping process often occurred in conjunction with shifts in the position of one or both myofibrils, followed by the reassociation of adjacent Z lines (Fig. 12 *d*). The combination of dissociation, changes in position, and reassociation resulted in improved alignment of the sarcomeres of the two myofibrils.

Not all shifts in myofibril position were coupled to the breaking of associations. Often, the shifts of one myofibril pulled or deformed neighboring myofibrils (e.g., Fig. 4). These movements frequently initiated at distant points along

a myofibril and then propagated along it. In some cases, fusion of single cells or myotubes, or rapid increases in the size or number of myofibrils seemed to be responsible for the movement of myofibrils and even of nuclei. However, movement of myofibrils was observed even in relatively mature cells where large numbers of myofibrils were already aligned (e.g., Fig. 10).

Discussion

Fluorescently labeled alpha-actinin has previously been injected into several cell types, including skeletal muscle (23, 33), cardiac muscle (26), fibroblasts (12, 23, 26), and epithelial cells (27). In every case, its distribution mimics closely the localization of endogenous alpha-actinin. Our present observations further suggest that microinjected alpha-actinin does not alter the developmental program of cultured chick myotubes. Thus, fluorescent analogue cytochemistry is a reliable method for following the changing distribution of alpha-actinin and structures containing alpha-actinin during myogenesis.

Formation of Z Lines

We have demonstrated that Z lines develop through the coalescence and condensation of diffuse bead-like aggregates of alpha-actinin. Previous studies using antibodies to alpha-

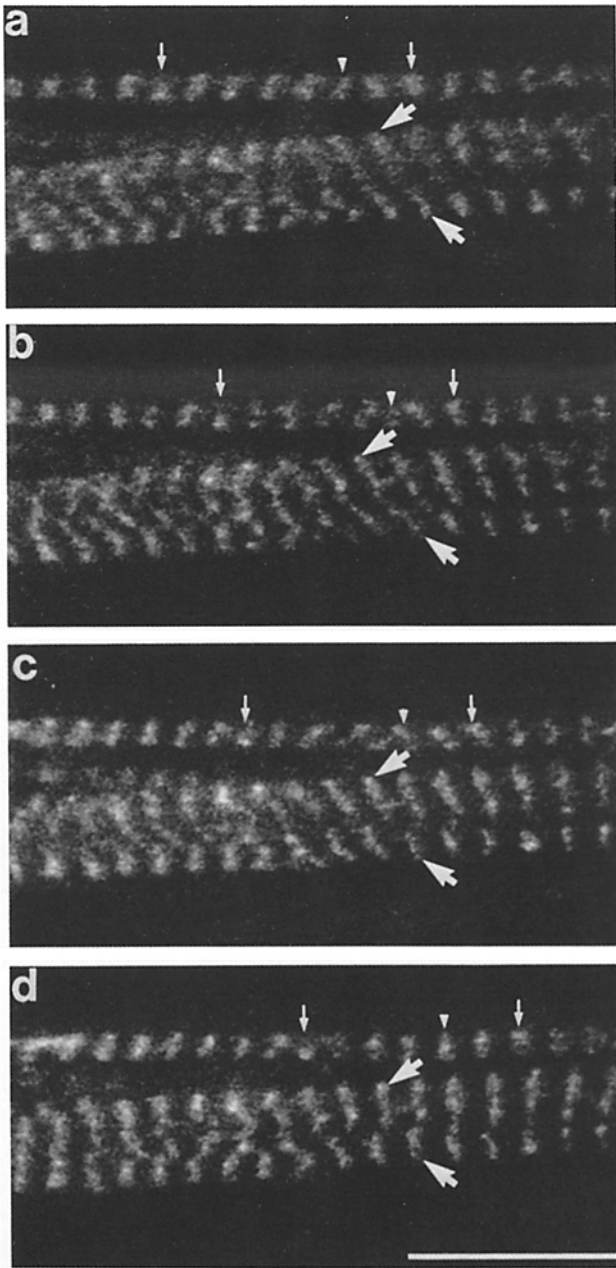


Figure 12. Adjustment of Z-line alignment in a 7-d myotube injected with rhodamine alpha-actinin. The small arrows indicate the same two Z lines throughout the time series. The large arrows indicate the ends of a Z line which is at a sharp angle to the myofibril at time 0 (a). 2 h later (b), the myofibril has split into two branches just to the right of the lower large arrow, with the result that the associated sarcomeres of the two branches “unzip.” The Z lines have also become anti-periodic. At 3½ h (c), the split has extended through the Z line indicated by the large arrows, and by 6 h (d), the two parts of the Z line have each realigned with parts of the adjacent myofibrils. The Z lines are also now perpendicular to the long axis of the myotube. The arrowhead indicates a Z line which is well-defined in a. By b, adjacent Z lines on the same myofibril have apparently collapsed toward the Z line indicated by the arrowhead. By c, the Z line has merged with its neighbor on the left to form an upside down V-shaped structure. At the final time point (d), the Z line has merged completely with its neighbor. Bar, 10 μm .

actinin or fluorescently labeled alpha-actinin applied to glycerinated cell models have also indicated that alpha-actinin in embryonic muscle cells is localized in bead-like structures, similar to those described here (19, 31, 32). Even in the most mature cells that we have examined, the Z lines were still composed of a narrow string of alpha-actinin-containing beads. The coalescence of diffuse aggregates (Fig. 3) and the recruitment of individual aggregates into existing Z lines (Fig. 8) provide direct evidence that these bead-like structures act as building blocks of Z lines. In addition, since previous observations indicate that Z bodies are almost always associated with thin filaments (13, 14, 21), movement of these alpha-actinin-containing beads presumably also involves movement or even active interactions of actin and myosin filaments.

We have also detected a significant decrease in the width of Z bands/Z lines with time. Changes in the width of Z lines during development have also been reported in several systems. In *Xenopus* myotomal cells, early Z bands are $\sim 0.2\text{-}\mu\text{m}$ wide in electron micrographs, whereas more mature ones are $0.05\text{--}0.1\text{-}\mu\text{m}$ wide (29). Similarly, Z bands/Z lines in larval newt skeletal muscle (21), rodent cardiac muscle (24), and embryonic chick myotomal muscle (1) are also relatively wide.

The actual molecular mechanisms responsible for the condensation of alpha-actinin in Z bands are not known. Although alpha-actinin can self associate (31), other proteins may also be involved. However, an increase in the alignment of fibrils too small to resolve may contribute to this process as well, since incomplete alignment of very small fibrils could make Z bands appear wide.

We have demonstrated two different ways in which Z lines can grow in length (perpendicular to the axis of myotubes). The addition of detectable structures to Z lines occurs only at the earlier stages of sarcomerogenesis when less developed structures lie alongside myofibrils. The other method of lateral growth, the addition of alpha-actinin directly to existing Z lines without the involvement of visible intermediate structures, occurs at all stages in our experiments and probably continues into postnatal life (28).

Sarcomeric Periodicity

Some authors have proposed that the closely spaced, linear arrays of beads observed in very immature muscle cells move apart to establish sarcomeric periodicity in mature cells (31, 32). In developing insect muscle (6) and chick myotomal muscle (1, 2), the length of sarcomeres has also been reported to increase, possibly through filament growth or stretching. Other authors, however, have reported that newly formed sarcomeres have essentially the same length as mature sarcomeres, even though they lack a discrete H zone (29). In our experiments, we have not detected a consistent, direct increase in sarcomere length during this specific period of development. However, we cannot rule out the possibility that the distance between the alpha-actinin containing beads may increase at very early stages of development, before the initiation of our time-lapse recording.

We have, however, detected a decrease in the variability of sarcomere periodicity, which involved both increases and decreases in the length of individual sarcomeres, such that the mean sarcomere length changed very little. It is possible

that these changes are related to a transition from variable lengths of actin filaments into a more uniform length (37).

Dynamics and Alignment of Myofibrils

Our observations also highlight the high degree of plasticity of myofibrils and other structures in developing myotubes. Although almost all fusion has ceased in these cultures by the beginning of observation, nuclei and myofibrils still move longitudinally, and, to a lesser extent, laterally in the myotubes. In addition, neighboring myofibrils underwent constant lateral associations and dissociations. The combination of shifts in the relative position of myofibrils and the formation and breakage of lateral associations between sarcomeres facilitates the alignment of sarcomeres through a trial and error process. Only in extensively cross-striated myotubes from 7 d or older cultures did major shifts in myofibril position become less common and did nuclei gain an elongated shape and peripheral position. These cells were generally very densely packed with myofibrils and it is likely that they correspond to the stages at which desmin begins to show a Z line periodicity (15).

What influences the movements of myofibrils and dictates correct alignment? Some authors have suggested that contraction could be important for alignment (35). Our unpublished time-lapse studies of cultured chick cardiac muscle cells have also suggested a correlation between contraction and alignment. However, although contraction does occur in uninervated myotube cultures, frequent or rhythmic contraction does not, so it is not clear to what extent contraction can contribute to alignment here. Other authors have postulated that the tension developed by cell-substratum attachment could be an organizing force (18, 34, 38). For example, myotubes formed in suspension culture contain a jumble of unaligned myofibrils until they are allowed to attach to a substrate. Then the myofibrils in the spreading processes rapidly align (30). In addition, tension-producing conditions, such as the steady stretching of the substratum, cause myotubes to be perpendicularly oriented to the direction of the stretch (38). Possibly, such forces place poorly aligned associations under greater stress than well-aligned associations, with the result that poorly aligned associations would be less stable and shorter lived. Eventually, almost all misaligned or poorly aligned associations would be replaced and well aligned myofibrils would predominate.

The authors wish to thank S. Stickel for reading the manuscript.

This study was supported by National Science Foundation Grant DCB-8510673, and by the Muscular Dystrophy Association.

Received for publication 5 June 1986, and in revised form 11 August 1986.

References

1. Allen, E. R. 1973. Sarcomere formation in chick striated muscle. *Z. Zellforsch. Mikrosk. Anat.* 145:167-170.
2. Allen, E. R. 1978. Development of vertebrate skeletal muscle. *Am. Zool.* 18:101-111.
3. Allen, R. E., M. H. Strohman, D. E. Goll and R. M. Robson. 1979. Accumulation of myosin, actin, tropomyosin and alpha-actinin in cultured muscle cells. *Dev. Biol.* 69:655-660.
4. Amato, P. A., E. R. Unanue, and D. L. Taylor. 1983. Distribution of actin in spreading macrophage: a comparative study on living and fixed cells. *J. Cell Biol.* 96:750-761.
5. Antin, P. B., S. Tokunaka, V. T. Nachmias, and H. Holtzer. 1986. Role of stress fiber like structures in assembling nascent myofibrils in myosheets recovering from exposure to ethyl methanesulfonate. *J. Cell Biol.* 102:1464-1479.

6. Auber, J. 1969. La myofibrillogenese du muscle strie. I. *Insectes. J. Microscopie.* 8:197-232.
7. Bush, W. A., M. H. Stromer, D. E. Goll, and A. Suzuki. 1972. Ca⁺⁺-specific removal of Z-lines from rabbit muscle. *J. Cell Biol.* 52:367-381.
8. Chowrashi, P. K., and F. A. Pepe. 1982. The Z-band: 85,000-dalton amorphin and alpha-actinin and their relation to structure. *J. Cell Biol.* 94:565-573.
9. Croop, J., Y. Toyama, A. A. Dlugosz, and H. H. Holtzer. 1980. Selective effects of phorbol 12-myristate 13-acetate on myofibrils and 10 nm filaments. *Proc. Natl. Acad. Sci. USA.* 77:5273-5277.
10. Devlin, R. B., and C. P. Emerson, Jr. 1978. Coordinate regulation of contractile protein synthesis during myofibrillar differentiation. *Cell.* 13:599-611.
11. Doetschman, T. C., and H. M. Eppenberger. 1984. Comparison of M-line and other myofibril components during reversible phorbol ester treatment. *Eur. J. Cell Biol.* 33:265-274.
12. Feramisco, J. R., and S. H. Blose. Distribution of fluorescently labeled alpha-actinin in living and fixed fibroblasts. *J. Cell Biol.* 86:608-615.
13. Fischman, D. A. 1970. The synthesis and assembly of myofibrils in embryonic muscle. *Curr. Top. Dev. Biol.* 5:235-280.
14. Fischman, D. A. 1972. Development of striated muscle. In *The Structure and Function of Muscle*, 2nd ed., Vol. 1. G. H. Bourne, editor. Academic Press, Inc., NY. 75-148.
15. Gard, D. L., and E. Lazarides. 1980. The synthesis and distribution of desmin and vimentin during myogenesis in vitro. *Cell.* 19:263-275.
16. Goll, D. G., A. Suzuki, J. Campbell, and G. R. Holmes. 1972. Studies on purified alpha-actinin. *J. Mol. Biol.* 67:469-488.
17. Hill, C. S., and L. F. Lemanski. 1985. Immunoelectron microscopic localization of alpha-actinin and actin in embryonic hamster heart cells. *Eur. J. Cell Biol.* 39:300-312.
18. Isobe, Y., and Y. Shimada. 1983. Myofibrillogenesis in vitro as seen with the scanning electron microscope. *Exp. Cell Res.* 231:481-494.
19. Jockusch, H., and B. M. Jockusch. 1980. Structural organization of the Z-line protein, alpha-actinin, in developing skeletal muscle cells. *Dev. Biol.* 75:231-238.
20. Kaneko, H., M. Okamoto, and K. Goshima. 1984. Structural change of myofibrils during mitosis of newt embryonic myocardial cells in culture. *Exp. Cell Res.* 153:483-498.
21. Kelly, D. E. 1969. Myofibrillogenesis and Z-band differentiation. *Anat. Rec.* 163:403-426.
22. Konisberg, I. R. 1979. Skeletal myoblasts in culture. *Methods Enzymol.* 58:511-527.
23. Kreis, T. E., and W. Birchmeier. 1980. Stress fiber sarcomeres of fibroblasts are contractile. *Cell.* 22:555-561.
24. Markwald, R. R. 1973. Distribution and relationship of precursor Z material to organizing myofibrillar bundles in embryonic rat and hamster ventricular myocytes. *J. Mol. Cell. Cardiol.* 5:341-350.
25. Masaki, T., M. Endo, and S. Ebashi. 1967. Localization of 6S component of alpha-actinin at Z-band. *J. Biochem. (Tokyo).* 62:630-632.
26. McKenna, N. M., J. B. Meigs, and Y.-L. Wang. 1985. Exchangeability of alpha-actinin in living cardiac fibroblasts and muscle cells. *J. Cell Biol.* 101:2223-2232.
27. Meigs, J. B., and Y.-L. Wang. 1986. Organization of alpha-actinin and vinculin induced by a phorbol ester in living cells. *J. Cell Biol.* 102:1430-1438.
28. Morkin, E. 1970. Post-natal muscle fiber assembly localizing of newly synthesized myofibrillar proteins. *Science (Wash. DC).* 167:1499-1501.
29. Peng, H. B., J. J. Wolosewick, and P. C. Cheng. 1981. The development of myofibrils in cultured muscle cells: a whole mount and thin-section electron microscopic study. *Dev. Biol.* 88:121-136.
30. Puri, C., M. Caravotti, J. C. Perriard, D. C. Turner, and H. M. Eppenberger. 1980. Anchorage independent muscle cell differentiation. *Proc. Natl. Acad. Sci. USA.* 77:5297-5301.
31. Sanger, J. W., B. Mittal, and J. M. Sanger. 1984. Analysis of myofibrillar structure and assembly using fluorescently labeled contractile proteins. *J. Cell Biol.* 98:825-833.
32. Sanger, J. W., B. Mittal, and J. M. Sanger. 1984. Formation of myofibrils in spreading chick cardiac myocytes. *Cell Motil.* 4:405-416.
33. Sanger, J. M., B. Mittal, M. Pochapin, J. S. Dome, and J. W. Sanger. 1985. Myogenesis in living cells microinjected with fluorescently labeled contractile proteins. *J. Cell Biol.* 101(5, Pt. 2):173a. (Abstr.)
34. Singer, R. H., and J. A. Pudney. 1984. Filament-directed intercellular contacts during differentiation of cultured myoblasts. *Tissue & Cell.* 16:17-29.
35. Taniguchi, M., and H. Ishikawa. 1982. In situ reconstitution of myosin filaments within the myosin-extracted myofibril in cultured skeletal muscle cells. *J. Cell Biol.* 92:324-332.
36. Tokuyasu, K. T., P. A. Maher, and S. J. Singer. 1984. Distribution of vimentin and desmin in developing chick myotubes in vivo. I. Immunofluorescence study. *J. Cell Biol.* 98:1961-1972.
37. Traeger, L., and M. A. Goldstein. 1983. Thin filaments are not of uniform length in rat skeletal muscle. *J. Cell Biol.* 96:100-103.
38. Vandenburg, H. H. 1982. Dynamic mechanical orientation of skeletal myofibers in vitro. *Dev. Biol.* 93:438-443.
39. Wang, K., J. R. Feramisco, and J. F. Ash. 1982. Fluorescent localization of contractile proteins in tissue culture cells. *Methods Enzymol.* 85:514-562.